



# Heavy precipitation events over East Africa in a changing climate: results from CORDEX RCMs

Obed M. Otega<sup>1,2</sup> · James Koske<sup>1</sup> · James B. Kung'u<sup>1</sup> · Enrico Scoccimarro<sup>3</sup> · Hussen S. Endris<sup>4</sup> · Malcolm N. Mistry<sup>5</sup>

Received: 17 December 2019 / Accepted: 22 May 2020 / Published online: 27 May 2020  
© Springer-Verlag GmbH Germany, part of Springer Nature 2020

## Abstract

The study assesses the performance of 24 model runs from five COordinated Regional climate Downscaling Experiment (CORDEX) regional climate models (RCMs) in simulating East Africa's spatio-temporal precipitation characteristics using a set of eight descriptors: consecutive dry days (CDD), consecutive wet days (CWD), simple precipitation intensity index (SDII), mean daily annual (pr\_ANN), seasonal (pr\_MAM and pr\_OND) precipitation, and representatives of heavy precipitation (90p) and very intense precipitation (99p) events. Relatively better performing RCM runs are then used to assess projected precipitation changes (for the period 2071–2099 relative to 1977–2005) over the study domain under the representative concentration pathway (RCP) 8.5 scenario. The performance of RCMs is found to be descriptor and scope specific. Overall, RCA4 (r1i1p1) forced by CNRM-CERFACS-CNRM-CM5 and MPI-M-MPI-ESM-LR, REMO2009 (r1i1p1) forced by MPI-M-MPI-ESM-LR, and RCA4 (r2i1p1) forced by MPI-M-MPI-ESM-LR emerge as the top four RCM runs. We show that an ensemble mean of the top four model runs outperforms an ensemble mean of 24 model simulations and ensemble means for all runs in an RCM. Our analysis of projections shows a reduction (increase) in mean daily precipitation for MAM(OND), an increase(decrease) in CDD(CWD) events, and a general increase in SDII and the width of the right tail of the precipitation distribution (99p–90p). An increase in SDII and 99p–90p implies a possibility of occurrence of heavy and extreme precipitation incidences by the end of the twenty-first century. Our findings provide important information to support the region's climate change adaptation and mitigation efforts.

**Keywords** Intraseasonal precipitation variability · CORDEX · Regional climate model · RCP 8.5 · Global warming

## 1 Introduction

Precipitation in East Africa (EA) is quite variable in both time and space (e.g. Opiyo et al. 2014; Kiros et al. 2017; Otega 2017). While the region tends to experience more

deficit than surplus precipitation events, major heavy precipitation events have been recorded over time which, often, lead to massive losses in life and property (e.g. Kilavi et al. 2018). An assessment of several climate indices done by Omundi et al. (2014) pointed towards a general decrease in historical precipitation trends over EA. Déqué et al. (2017) assessed the impact of +2° warming on tropical Africa's climate using several regional climate models (RCMs). Their assessment showed a possibility of increased extreme precipitation events by 2100. Further, precipitation projections over the Greater Horn of Africa under 1.5 °C and 2 °C global warming indicate (i) uncertainty in changes in precipitation, (ii) increasing dry spells, and (iii) decreasing wet spells over the region by 2100 (Osima et al. 2018). However, none of these studies have made an in-depth assessment of (1) the capability of RCMs (analysing individual model runs) to reproduce EA's spatial and temporal precipitation extremes

✉ Obed M. Otega  
obed.matundura@gmail.com

<sup>1</sup> School of Environmental Studies, Kenyatta University, Nairobi, Kenya

<sup>2</sup> The African Academy of Sciences, Nairobi, Kenya

<sup>3</sup> Fondazione CMCC Centro Euro-Mediterraneo Sui Cambiamenti Climatici, Bologna, Italy

<sup>4</sup> IGAD Climate Prediction and Applications Centre, Nairobi, Kenya

<sup>5</sup> Department of Economics, Ca' Foscari University of Venice, Venice, Italy

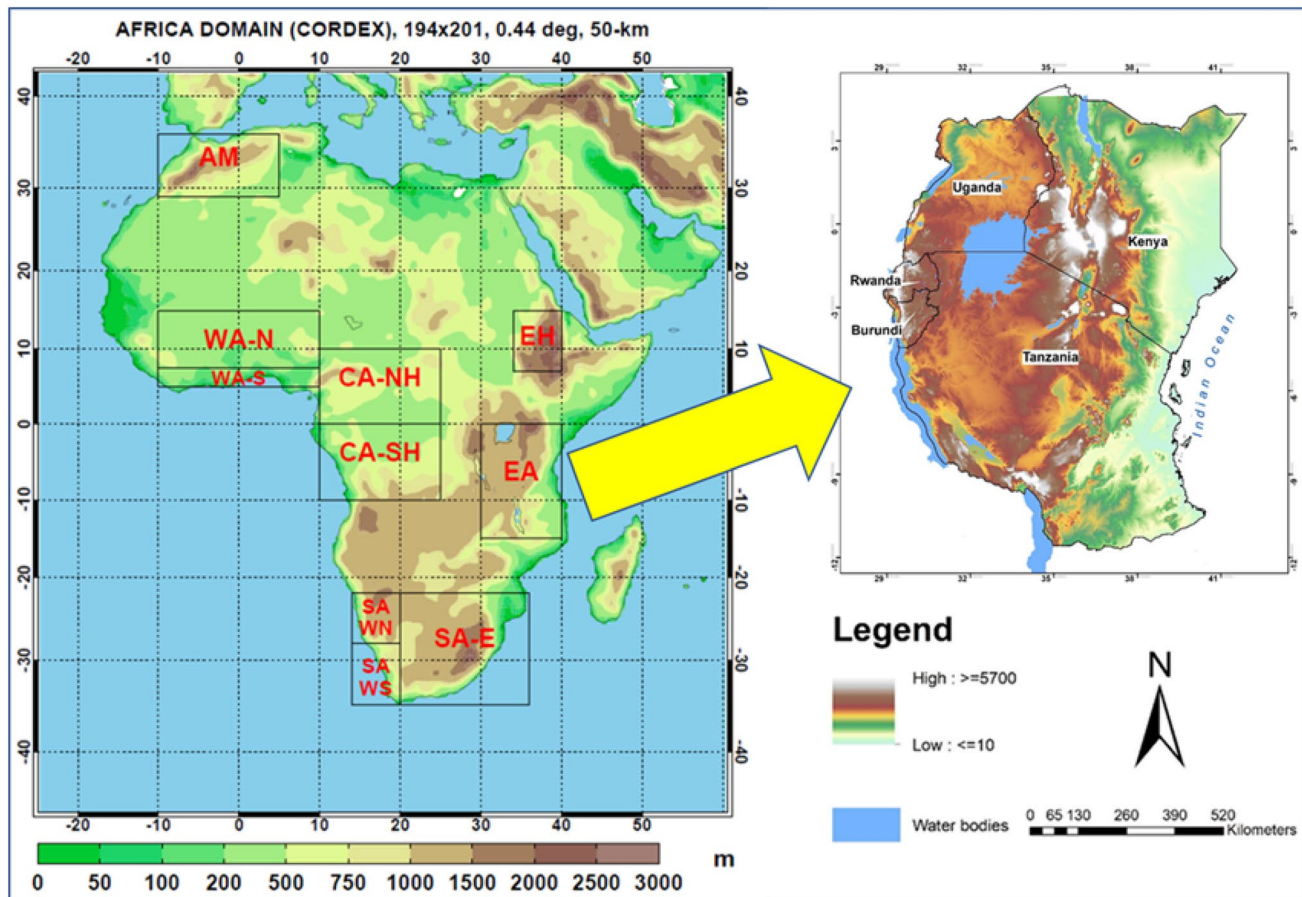


**Fig. 1** Map of the study area (adapted from Kim et al. 2014)

and (2) conclusive projections of occurrence, intensity, and frequency of extreme precipitation by 2100.

The current study, therefore, seeks to contribute to efforts being made to enhance the understanding of potential occurrence of heavy and extreme precipitation events to inform more adequate disaster preparedness and mitigation strategies over EA. Specifically, the study assesses the performance of 24 runs from CORDEX RCMs in simulating EA's spatial and temporal precipitation variability and analyses projections for changes in EA's heavy and extreme precipitation events under a global warming scenario (RCP 8.5, Moss et al. 2010). The rest of the paper is structured into data and methods (2), results and discussion (3), and summary and conclusions (4).

## 2 Data and methods

### 2.1 Study area

The study focused on the East Africa (EA) sub-region of CORDEX-Africa domain (Favre et al. 2011; Kim et al.

2014). The EA sub-region, extending from 30° to 40° East and 0° to 15° South, experiences two main rainy seasons namely March to May (MAM) and October to December (OND, Favre et al. 2011). A slight extension of the CORDEX-EA sub-region was made to cover five countries that are part of the East African Community (EAC) namely Kenya, Uganda, Tanzania, Rwanda, and Burundi (Fig. 1).

### 2.2 Data

#### 2.2.1 RCM data

Total daily precipitation data (not bias corrected and in its native form) from five CORDEX-Africa RCMs (Table 1) at 0.44° (~50 km at the equator) gridded resolution were used in the study. Specifically, we used 24 realizations of precipitation from RCMs (described in detail by Nikulin et al. 2012) forced by general circulation models (GCMs) resulting from single or multiple ensemble runs. The GCMs are part of the fifth phase of the Coupled Model Intercomparison Project (CMIP5, Meehl and Bony 2011).

**Table 1** List of RCMs used in study. The data were accessed in August 2019 from the Deutsches Klimarechenzentrum (DKRZ, <https://bit.ly/2RoList>)

Institute	RCM		Herein-after	Ensemble	Driving model
Climate Limited-Area Modelling (CLM) Community	CLMcom COSMOCLM (CCLM4)	CCLM4	r1i1p1	MOHC-HadGEM2-ES MPI-M-MPI-ESM-LR CNRM-CERFACS-CNRM-CM5	
Max Planck Institute (MPI), Germany	MPI-CSC-REMO2009	REMO2009	r12i1p1 r1i1p1	ICHEC-EC-EARTH ICHEC-EC-EARTH MPI-M-MPI-ESM-LR	
Sveriges Meteorologiska och Hydrologiska Institut (SMHI), Sweden	SMHI Rossby Center Regional Atmospheric Model (RCA4)	RCA4	r1i1p1	CSIRO-QCCCE-CSIRO-Mk3-6-0 MIROC-MIROC5 MOHC-HadGEM2-ES NCC-NorESM1-M MPI-M-MPI-ESM-LR IPSL-IPSL-CM5A-MR NOAA-GFDL-GFDL-ESM2M CCCma-CanESM2 CNRM-CERFACS-CNRM-CM5 ICHEC-EC-EARTH	
Koninklijk Nederlands Meteorologisch Instituut (KNMI), Netherlands	KNMI Regional Atmospheric Climate Model, version 2.2 (RACMO2.2T)	RACMO22T	r1i1p1	ICHEC-EC-EARTH r2i1p1 r3i1p1	MOHC-HadGEM2-ES ICHEC-EC-EARTH MOHC-HadGEM2-ES
Danish Meteorological Institute (DMI)	DMI-HIRHAM5	HIRHAM5	r3i1p1 r1i1p1	ICHEC-EC-EARTH NCC-NorESM1-M	

### 2.2.2 Reference data

The daily Climate Hazards Group InfraRed Precipitation with Station data (CHIRPS) version 2.0 was used as a reference dataset. CHIRPS data incorporates satellite imagery (at 0.05° and 0.25° resolution) with in-situ station data resulting in a gridded precipitation time series—available from 1981 to near-present (Funk et al. 2015). The other reference dataset utilized is the Tropical Applications of Meteorology using SATellite and ground-based observations, version 3 (TAMSAT3, Maidment et al. 2017). Both datasets have been validated for EA and found to be suitable for use as reference datasets (Dinku et al. 2018).

Three other data products were also considered namely the daily global historical climatology network (GHCN-Daily, Menne et al. 2012); the global precipitation climatology project (GPCP, Huffman et al. 2009); and the Multi-Source Weighted-Ensemble Precipitation (MSWEP, Beck et al. 2019). While GHCN-Daily had significant data gaps for our study area, GPCP data range from 1996 to near present, thus falling outside our study period (1989–2005). Our data request to the creators of MSWEP, a global gridded

precipitation dataset at 0.1° resolution generated by optimally merging various satellite, reanalysis estimates, and gauge data, went unanswered. Hence, CHIRPS and TAMSAT3 were used as reference data. Due to differing resolutions of model and reference datasets, computations on data were done on their native grids and resolutions (as in Diaconescu et al. 2015) before bilinearly interpolating the processed files (Zhou et al. 2017) to facilitate comparison between model simulations and reference data.

### 2.3 Methods

An evaluation of the performance of RCMs in simulating EA's spatial and temporal precipitation characteristics (for the period 1983–2005) was done using simulations from five CORDEX-Africa RCMs forced by GCMs. The period 1983 to 2005 was chosen to correspond to data availability for reference data (CHIRPS and TAMSAT3) which are available from 1981 and 1983 to near present, respectively. It also corresponds to historical simulations of the CORDEX-Africa RCMs (up-to year 2005).

**Table 2** Climate indices and precipitation statistics used as descriptors of a rainy season in the study

Descriptor	Acronym	Description	Unit
Simple precipitation intensity index	SDII	Mean precipitation amount on a wet day. Let $RR_{ij}$ be the daily precipitation amount on a wet day $w$ ( $RR \geq 1 \text{ mm}$ ) in period $j$ . If $W$ represents the number of wet days in $j$ then the simple precipitation intensity index $SDII_j = \sum (RR_{wj})/W$	mm/day
Consecutive dry days	CDD	Maximum length of dry spell ( $RR < 1 \text{ mm}$ ). Let $RR_{ij}$ be the daily precipitation amount on day $i$ in period $j$ . Count the largest number of consecutive days where $RR_{ij} < 1 \text{ mm}$	days
Consecutive wet days	CWD	Maximum length of wet spell, maximum number of consecutive days with $RR \geq 1 \text{ mm}$ : Let $RR_{ij}$ be the daily precipitation amount on day $i$ in period $j$ . Count the largest number of consecutive days where: $RR_{ij} \geq 1 \text{ mm}$	days
Mean daily precipitation for MAM season	pr_MAM	For every adjacent sequence $t_1, \dots, t_n$ of timesteps of the same year it is: $o(t, x) = \text{mean}\{i(t', x), t_1 < t' \leq t_n\};$ computed for March–May of every year in the series	mm/day
Mean daily precipitation for OND season	pr_OND	For every adjacent sequence $t_1, \dots, t_n$ of timesteps of the same year it is: $o(t, x) = \text{mean}\{i(t', x), t_1 < t' \leq t_n\};$ computed for October–December of every year in the series	mm/day
Mean daily precipitation in a year	pr_ANN	For every adjacent sequence $t_1, \dots, t_n$ of timesteps of the same year it is: $o(t, x) = \text{mean}\{i(t', x), t_1 < t' \leq t_n\};$ computed for every year in the series	mm/day
Representative of heavy precipitation events	90p	For every adjacent sequence $t_1, \dots, t_n$ of timesteps of the same year it is: $o(t, x) = \text{pth percentile}\{i(t', x), t_1 < t' \leq t_n\};$ here computed for the 90th percentile. For this study, 90p represents the threshold for identifying heavy precipitation events	days
Representative of very intense precipitation events	99p	For every adjacent sequence $t_1, \dots, t_n$ of timesteps of the same year it is: $o(t, x) = \text{pth percentile}\{i(t', x), t_1 < t' \leq t_n\};$ here computed for the 99th percentile. For this study, 99p represents very intense precipitation events	days

The performance of RCMs was measured against a set of eight descriptors (Table 2); representative of both moderate to extreme precipitation events (precipitation-based indices and annual precipitation statistics). CDD, CWD, and SDII are climate indices (Peterson et al. 2001) considered to be highly sensitive to global warming and climate change and are widely used in extreme precipitation identification and monitoring (e.g. Jiang et al. 2015; Sillmann et al. 2013; Zhou et al. 2014; Osima et al. 2018).

Ranking of the performance of RCMs in simulating EA's precipitation was done using two criteria the first of which is ranking models based on their performance in simulating the spatial characteristics of the eight descriptors relative to observations. Here, spatial correlation coefficients (PCC) for each model were computed and ranked using detrended data. Secondly, models were ranked based on their performance in simulating year-to-year variability of the eight descriptors in comparison to observations. Here, inter-annual variability skill scores (IVS; Chen et al. 2011) were computed using detrended data as follows (Eq. 1):

$$IVS = \left( \frac{STD_m}{STD_o} - \frac{STD_o}{STD_m} \right)^2; \quad (1)$$

where  $STD_o$  and  $STD_m$  represent the standard deviation for observations and models, respectively. An IVS value of 0 implies that  $STD_o$  is equal to  $STD_m$  and the closer an IVS value is to 0 the better its skill in simulating the inter-annual variability (Chen et al. 2011).

A comprehensive rating index (defined in Jiang et al. 2015) was used to rank the performance of RCMs as follows:

$$MR = 1 - \frac{1}{nm} \sum_{i=1}^n rank_i; \quad (2)$$

where  $n$  is the number of descriptors and  $m$  the number of RCMs. The model with an MR value closest to 1 gives the best skill of simulation compared to other models under consideration (Jiang et al. 2015).

A scatter diagram using model run rankings (based on both IVS and PCC) was plotted to facilitate comparison. The best performing model runs are found in the first quadrant (Q1) while the worst performing runs are found in the Q3 of the scatter plot. The best four model runs (based on MR) and their ensemble mean were used to analyse the output for model projections. Specifically, changes in future (period 2071 to 2099) precipitation characteristics (for all the eight descriptors) relative to the baseline (period 1977 to 2005) were analysed. The analysis was done using projections made under the RCP 8.5 forcing (also referred to as ‘worst case scenario’) which assumes a net radiation at the top of the atmosphere of 8 W/m<sup>2</sup> by the year 2100 (Moss et al. 2010).

Additionally, the width of the right tail distribution of precipitation events, represented as the difference between the 99th and the 90th percentiles (99p–90p), was used to assess past and future heavy and very intense precipitation events over EA. Here, the 99p represents very intense precipitation while the 90p represents the threshold for identifying heavy precipitation events. The percentiles were computed by aggregating daily precipitation values of the period under study over each grid cell (as in Scoccimarro et al. 2013, 2016).

### 3 Results and discussions

#### 3.1 Model performance evaluation

##### 3.1.1 Climatology

A plot of daily mean precipitation (Fig. 2) shows a generally good agreement between RCMs and observations in simulating spatial precipitation characteristics over EA. Areas over Uganda (30° E–33° E and 1° S–3.5° N) record the highest mean daily precipitation (at both annual and seasonal scales) while northern Kenya (34° E–41° E and 0° N–4° N) records the lowest mean daily precipitation. Southern and western parts of Tanzania show more average daily precipitation amounts compared to areas in central and northern Tanzania. Areas surrounding Lake Victoria (around 33° E, 2° S), including Rwanda and Burundi, record the highest mean daily precipitation exceeding 6 mm/day in some areas, during MAM season. The multi-model ensemble mean shows a slight under-approximation of annual (ANN) and MAM mean daily precipitation and daily precipitation events with precipitation amounts exceeding 90th and 99th percentiles (90p and 99p, respectively). The ensemble mean tends to give a slight over-approximation of the OND mean daily precipitation for the region.

A plot of the climatologies for extreme precipitation indices (not shown) shows areas over Uganda and around the

shows of Lake Victoria recording the least CDD compared to the rest of the study domain. The reverse is true for CWD. The highest daily precipitation intensity is recorded, generally, in areas east of the study domain (35° E–41° E) with a concentration in central Kenya and south-eastern Tanzania. Comparatively, the multi-model ensemble mean (24 runs) agrees with observations albeit with a slight over-estimation (under-estimation) of CDD and CWD over Uganda (Tanzania). The ensemble mean seems to under-represent SDII over the study domain. Markedly, the multi-model ensemble mean shows a better agreement with observations when reproducing CDD, CWD, and SDII at the 2.5 mm/day threshold<sup>1</sup> for a rainy day.

A plot of model biases, relative to observations, for all eight descriptors used in this study (Figs. 3, 4) show a general agreement between CHIRPS and TAMSAT3. Most of the study domain shows no significant differences between RCMs (ensemble mean) and observations. The RCMs seem to under-estimate ANN and MAM precipitation in areas over Uganda (north-west of the study domain) and around Lake Victoria (for MAM). The RCMs show a wet bias for OND season especially over north-western Tanzania (south-west of study domain). A minimal dry bias is shown for heavy precipitation events (90p) especially in areas over Uganda and western Tanzania. The RCMs show a dry bias especially over central Kenya and the western part of the study domain.

RCMs over-approximate/under-approximate CDD especially in several areas north/south of the study domain. They tend to over-approximate CWD in many parts west of the study domain and under-approximate SDII especially over the south and north-east of the study domain. Nonetheless, many areas over the study domain (especially over Kenya and Tanzania) show no significant differences between RCMs and observations. Generally, RCMs can adequately reproduce EA’s precipitation characteristics.

The recorded model under-approximation of ANN and MAM and the over-approximation of OND mean precipitation is consistent with similar studies over the study domain (e.g. Endris et al. 2013; Kisembe et al. 2018). These model biases could be as a result of EA’s complex climate systems (e.g. Nicholson and Kim 1997; Camberlin 2018) posing resolution challenges that RCMs have, probably, not yet been adequately configured to reproduce. Physical parameterization shortfalls for models have also been identified as potential reasons why some models over/under-approximate certain parameters (e.g. Dosio and Panitz 2016; Breil, Panitz and Schädler 2017). Additionally, we used a large ensemble of 24 runs in our analysis. Outliers in the multi-model

<sup>1</sup> In addition to the default threshold for a rainy day (1 mm/day), we used a higher threshold of 2.5 mm/day to facilitate comparison.

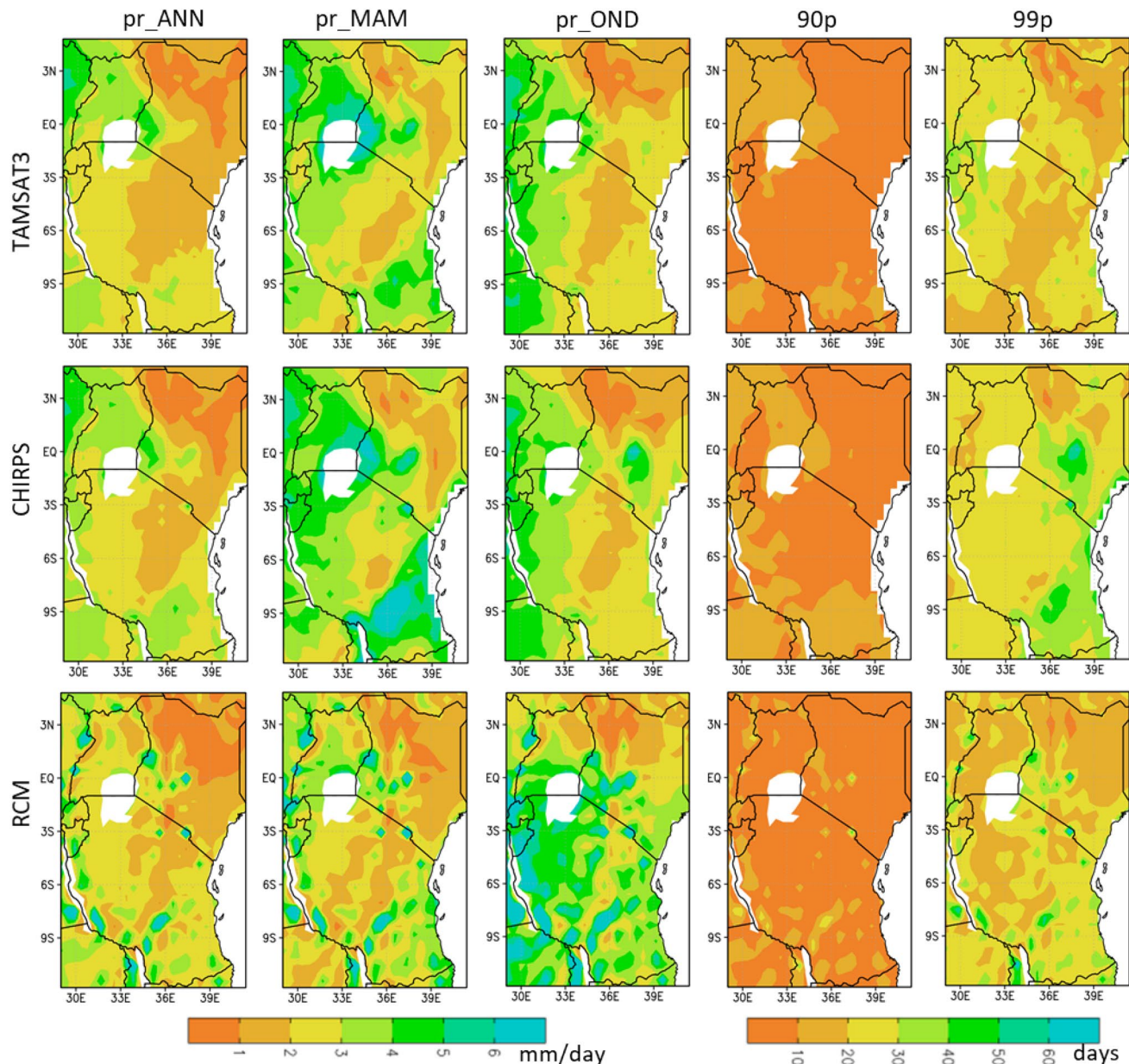


**Fig. 2** Climatology of seasonal (MAM and OND) and annual (ANN) mean daily precipitation and representatives of heavy precipitation (90p) and very intense precipitation (99p) events for observations (CHIRPS and TAMSAT3) and multi-model ensemble mean for RCMs forced by GCMs (bottom row), time-averaged for the period 1983–2005. Water bodies are shown in white

tions (CHIRPS and TAMSAT3) and multi-model ensemble mean for RCMs forced by GCMs (bottom row), time-averaged for the period 1983–2005. Water bodies are shown in white

ensemble may have contributed to the recorded model bias relative to observations.

### 3.2 Performance of RCMs in simulating E. African precipitation patterns

An analysis of the performance of 24 simulations from five CORDEX-Africa RCMs, ensemble means for each RCM, and a multi-RCM ensemble mean was done and ranked. Here, models were ranked from number 1 to  $m$ , where  $m$

is the number of model runs being assessed, for each of the eight descriptors. Overall performance (MR) per criteria (IVS and PCC) relative to observations (CHIRPS and TAMSAT3, respectively) were plotted in a scatter diagram (Figs. 5, 6). The best performing model runs are found in Q1 while the least performing models are in the Q3.

With CHIRPS as the reference data (Fig. 5), the top five model runs in simulating year-to-year precipitation characteristics over EA are RCA4 (r1i1p1) forced by MPI-M-MPI-ESM-LR, RCA4 (r1i1p1) forced by

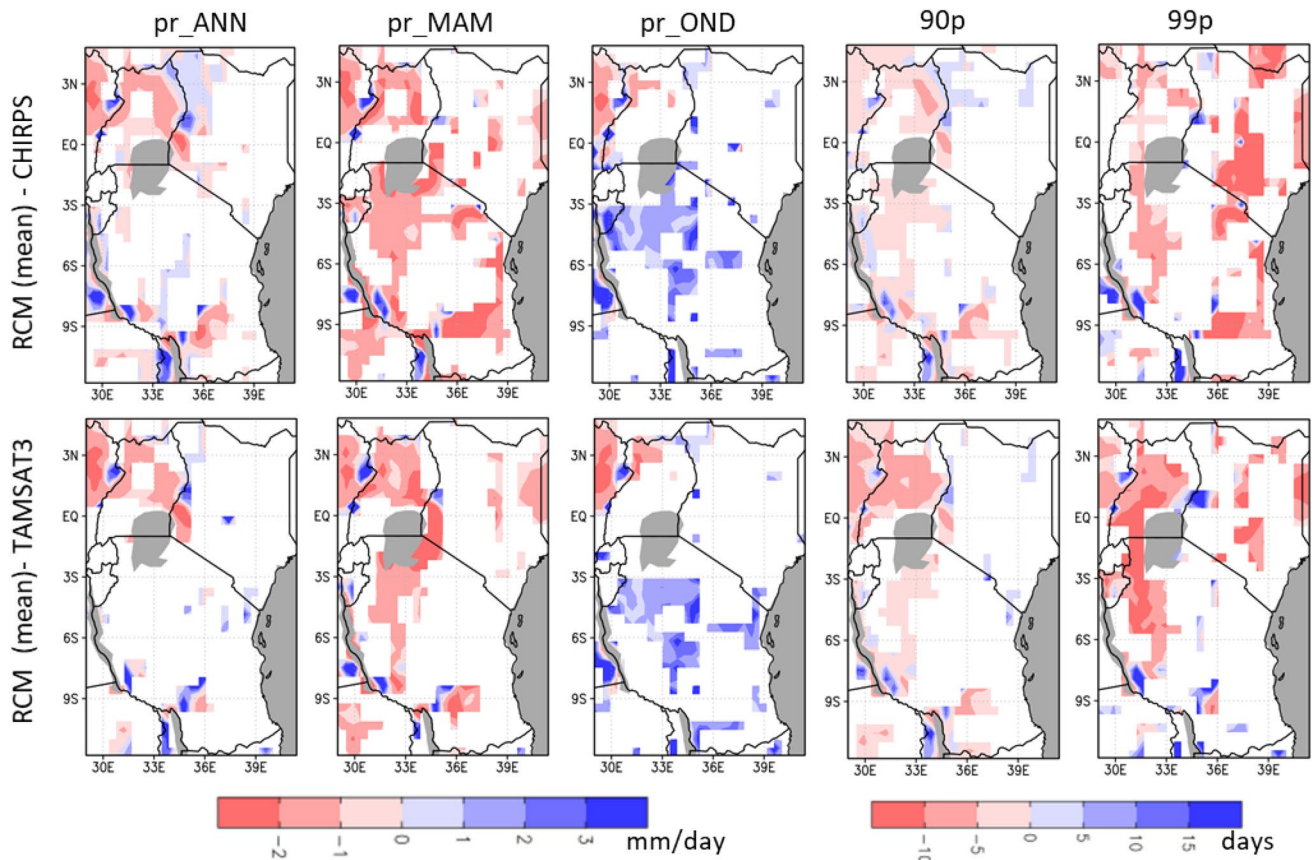


**Fig. 3** Significant (at 95% confidence level) differences between RCMs (ensemble mean) and observations (CHIRPS and TAMSAT3) averaged for the period 1983–2005. Water bodies are shown in grey. Positive (negative) values imply wet (dry) bias in RCM runs

CNRM-CERFACS-CNRM-CM5, HIRHAM5 (r1i1p1) forced by NCC-NorESM1-M, and RCA4 (r3i1p1) forced by MPI-M-MPI-ESM-LR, respectively. Spatial precipitation characteristics were best simulated by REMO2009 (r1i1p1) forced by MPI-M-MPI-ESM-LR, RCA4 (r1i1p1) forced by CNRM-CERFACS-CNRM-CM5, RCA4 (r1i1p1) forced by MPI-M-MPI-ESM-LR, RCA4 (r1i1p1) forced by ICHEC-EC-EARTH, and an ensemble mean for all GCMs driving RCA4, respectively. The best model runs for both criteria (IVS and PCC) are presented in Table 3. Overall, RCA4 (r1i1p1) forced by MPI-M-MPI-ESM-LR and RCA4 (r1i1p1) forced by CNRM-CERFACS-CNRM-CM5 emerged among the top model runs (relatively) in simulating both spatial and year-to-year precipitation characteristics over EA.

Unlike in the case of CHIRPS where models were concentrated in Q1, Q2, and Q4 (with none in the Q3), TAMSAT3 spreads the models in all quadrants (Fig. 6). The best model runs in simulating year-to-year characteristics are CCLM4 (r1i1p1) forced by CNRM-CERFACS-CNRM-CM5, RCA4 (r1i1p1) forced by MPI-M-MPI-ESM-LR, HIRHAM5 (r1i1p1) forced by NCC-NorESM1-M, CCLM4 (r1i1p1)

forced by ICHEC-EC-EARTH, and CCLM4 (r1i1p1) forced by MPI-M-MPI-ESM-LR. The best model runs for spatial characteristics were REMO2009 (r1i1p1) forced by MPI-M-MPI-ESM-LR, RCA4 (r1i1p1) forced by MPI-M-MPI-ESM-LR, RCA4 (r1i1p1) forced by IPSL-IPSL-CM5A-MR, RCA4 (r1i1p1) forced by CNRM-CERFACS-CNRM-CM5, and RCA4 (r2i1p1) forced by MPI-M-MPI-ESM-LR.

The top five model runs in simulating both spatial and temporal precipitation characteristics (with reference to TAMSAT3 data) are summarized in Table 4. The RCA4 (r1i1p1) forced by MPI-M-MPI-ESM-LR is the only model run that appeared among the top model runs in simulating both spatial and temporal precipitation characteristics of EA.

CHIRPS has been shown to give a better simulation of precipitation over EA than TAMSAT3 relative to observations (Dinku et al. 2018). In the current study, however, both CHIRPS and TAMSAT3 agreed on the top four model runs (Table 5) hence posing no need to choose between ranking results.

Previous studies done over our study domain suggest that a multi-model ensemble mean for RCMs forced by GCMs represent the climatology of precipitation over EA fairly well

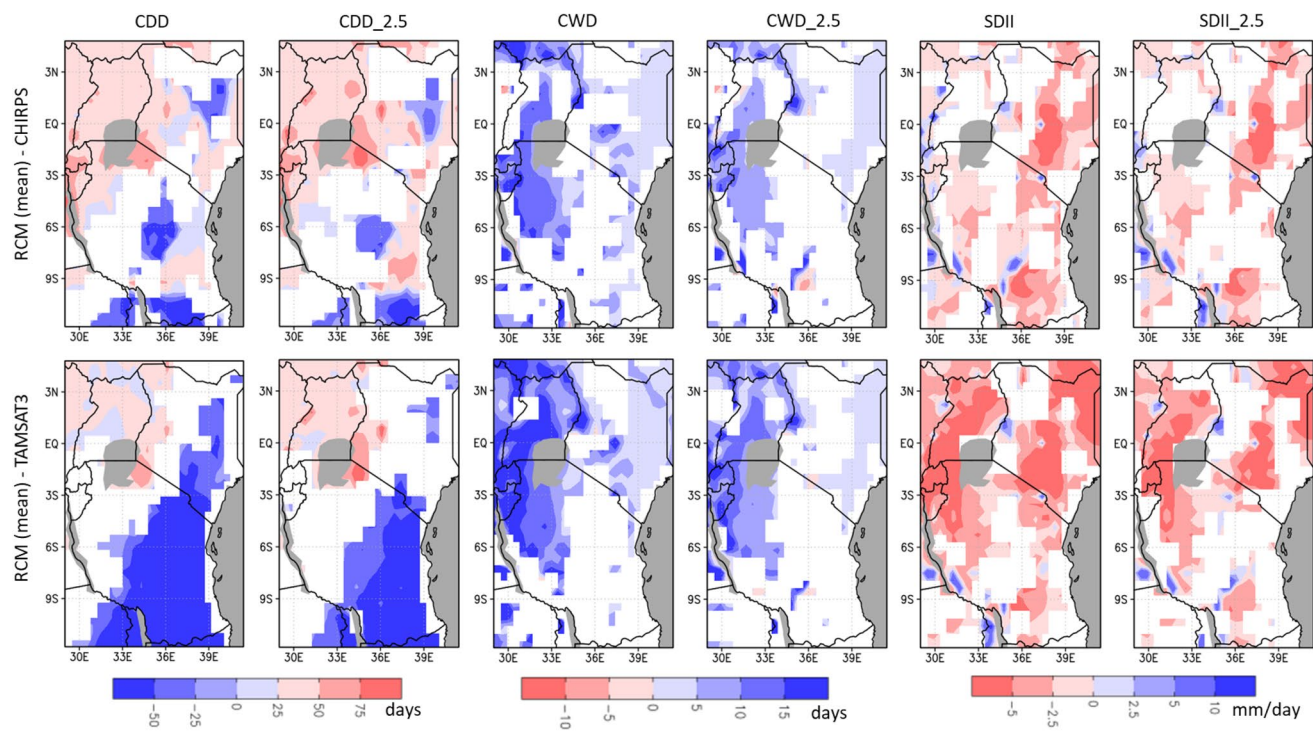


**Fig. 4** Same as Fig. 3 but for CDD, CWD, and SDII

(e.g. Endris et al. 2013; Shiferaw et al. 2018; Kisembe et al., 2018). However, these studies either used RCMs driven by re-analysis data or an ensemble mean of RCMs and not an ensemble mean of individual model runs. Our results show that an ensemble mean for the top four model runs performs better (ranked 5<sup>th</sup> after the top four model runs) than the multi-model ensemble mean for 24 model runs (Fig. 7). Comparatively, the multi-model ensemble mean (24 runs), and ensemble means for each RCM did not make it to the first quadrant. Therefore, a multi-model ensemble mean for a big set of model runs seems to be less competent in simulating both spatial and temporal precipitation characteristics for E. Africa. Our findings are consistent with Dosio et al. (2019) who, employing a large ensemble of CORDEX RCM runs, inferred that differences in RCM and GCM simulations make it difficult to subsample a particular model ensemble sufficient enough to produce a more robust result or reduce uncertainty.

The relative dismal performance of the multi-model ensemble mean (24 runs) in simulating EA's spatial and temporal precipitation characteristics could be attributed to various factors including a generally high variability in EA's year-to-year precipitation patterns (e.g. Endris et al. 2013). The complexity of EA's weather and climate caused by a blend of local and external systems such as topography and large inland water bodies (Nicholson 1997) could also be responsible for varied model simulations for EA. The current

resolution and parameterization of RCMs could be missing the impact of some of the local features hence leading the reduced performance in simulation (Dosio and Panitz 2016).

### 3.3 Heavy precipitation events over EA

An ensemble mean of the top four model runs listed in Table 5 was used to analyse future changes in precipitation using projections under the RCP8.5 scenario. A plot of climatology (Fig. 8) of the eight descriptors for the period 2071 to 2099 (FUT), compared to the historical period (1977 to 2005), show no major changes/slight decrease/slight increase for pr\_ANM/ pr\_MAM/ pr\_OND daily mean precipitation. 90p, 99p, CDD, CWD, and SDII show no major changes, a slight increase, a slight increase, a slight decrease, and a slight increase, respectively.

Using box plots (Figs. 9, 10), our results show no major changes in mean daily precipitation for ANN and a marginal drop of about 0.2 mm/day for MAM season. OND precipitation is projected to increase by about 0.5 mm/day to a daily average of 4 mm by 2100. A reduction in future MAM daily mean precipitation could be as a result of projected earlier onset/cessation dates for MAM precipitation hence potentially affecting (relative to the baseline) the MAM season length (Dunning et al. 2018; Wainwright et al. 2019).

Projections for CDD (Fig. 10) show an increase of about 10 days to around 105 days in a year compared to CWD that

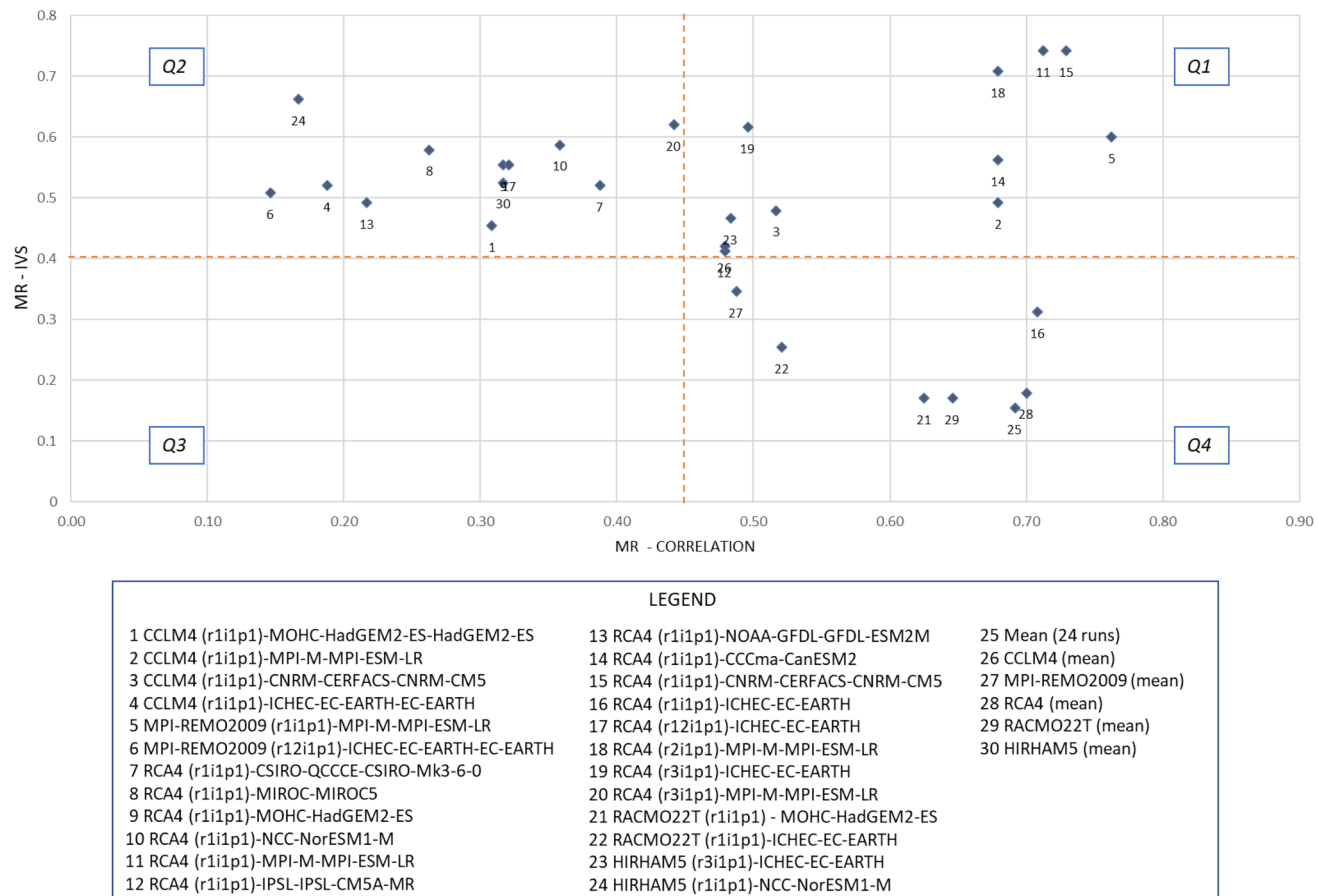


**Fig. 5** A scatter diagram showing model ranking (MR) based on IVS (y-axis) and correlation coefficients (x-axis), relative to CHIRPS data. The numbered dots represent models described in the legend

shows a marginal decrease of about 3 days to 8 days. SDII is projected to increase by about 3 mm/day to around 12 mm/day by the year 2100. Projections for heavy precipitation events (90p) show no changes while projections for very intense precipitation (99p) shows an increase of about five days in a year. The width of the right tail of the precipitation distribution (99p–90p) by about 5 days to an average of 20 days in a year.

A plot of changes in future precipitation (fut) relative to reference period (hist) shows no major changes for pr ANN and 90p (Fig. 11). No major changes are recorded for MAM season for most of Tanzania and Kenya except for areas over Uganda, Rwanda, Burundi with a reduction of up-to 2 mm/day. OND season shows no major changes over most of Tanzania and Burundi (southern part of the study domain) compared to the northern part of the study domain that shows an increase of up-to 2 mm/day. The outliers in each of the descriptors are not surprising given the spatial heterogeneity of the geographic area of our study, such as mountainous areas and flat lands (e.g. Nicholson and Kim 1997; Camberlin 2018). Many parts of northern Kenya and

Uganda are, largely, arid and semi-arid hence an increased mean daily precipitation could potentially increase arable land and, potentially, increase agricultural activities in EA. However, increased daily mean precipitation could result to flooding and landslides potentially causing socio-economic losses.

Our results complement other works that show a projected increase in OND seasonal precipitation over EA (e.g. Cook and Vizy 2013; Muhati et al. 2018; Gebrechorkos 2019) by showing the distribution at the daily timescale. An increased OND season length due to late precipitation onset and cessation (Wainwright et al. 2019) could be one of the reasons for the increased OND precipitation. A warming western Indian Ocean (Lazenby et al. 2018) potentially enhancing other conditions for OND precipitation could also be responsible for the projected increase in OND precipitation.

Projections for CDD (Fig. 11) show no major changes over Kenya, Uganda, and around Lake Victoria while most areas over Tanzania show a slight increase of up-to 25 days in a year. No significant changes are recorded for CWD in most of the study domain apart from some areas south and

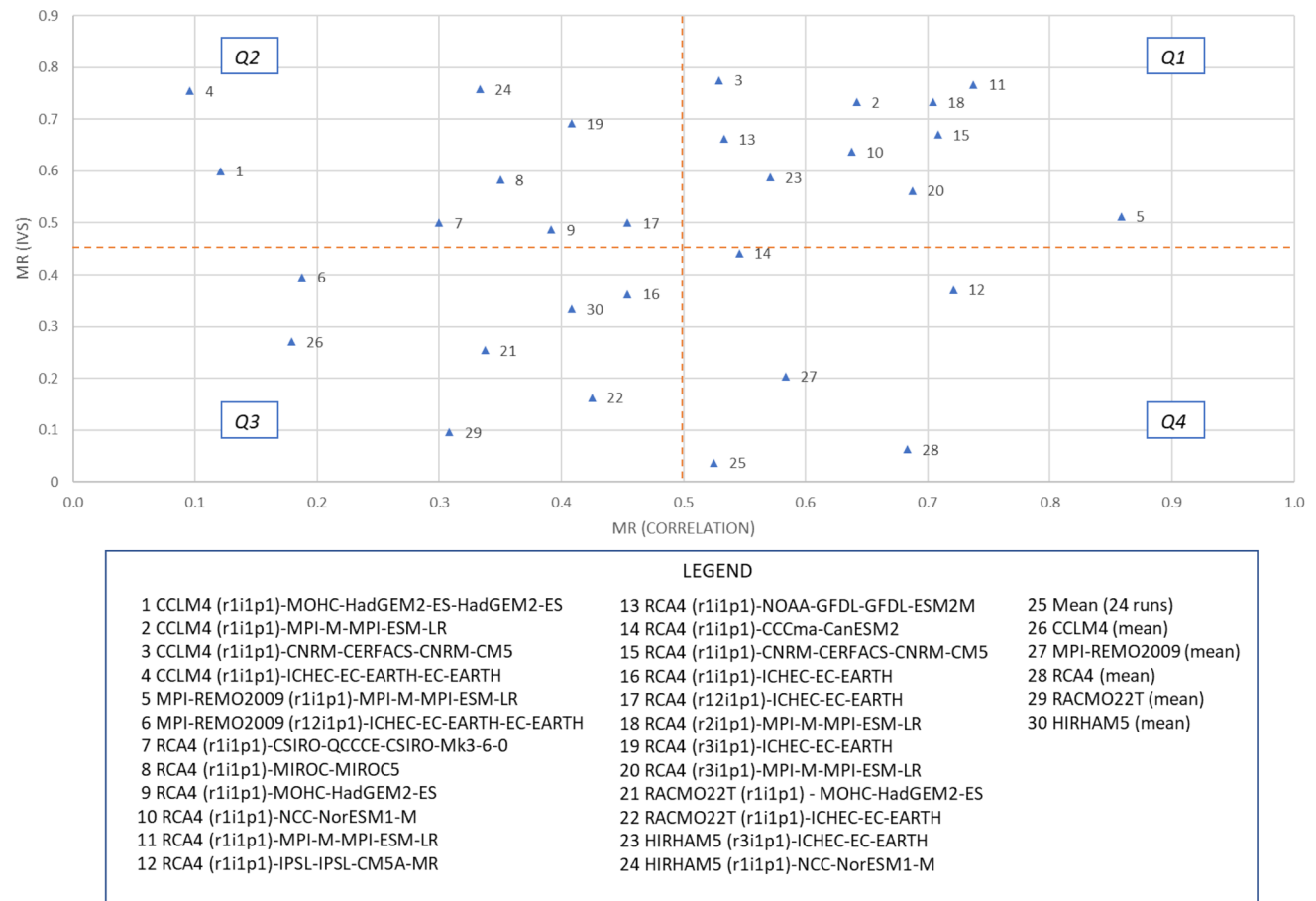


**Fig. 6** Same as Fig. 5 but using TAMSAT3 as reference data

**Table 3** Top five model runs in simulating both spatial and temporal precipitation characteristics with reference to CHIRPS

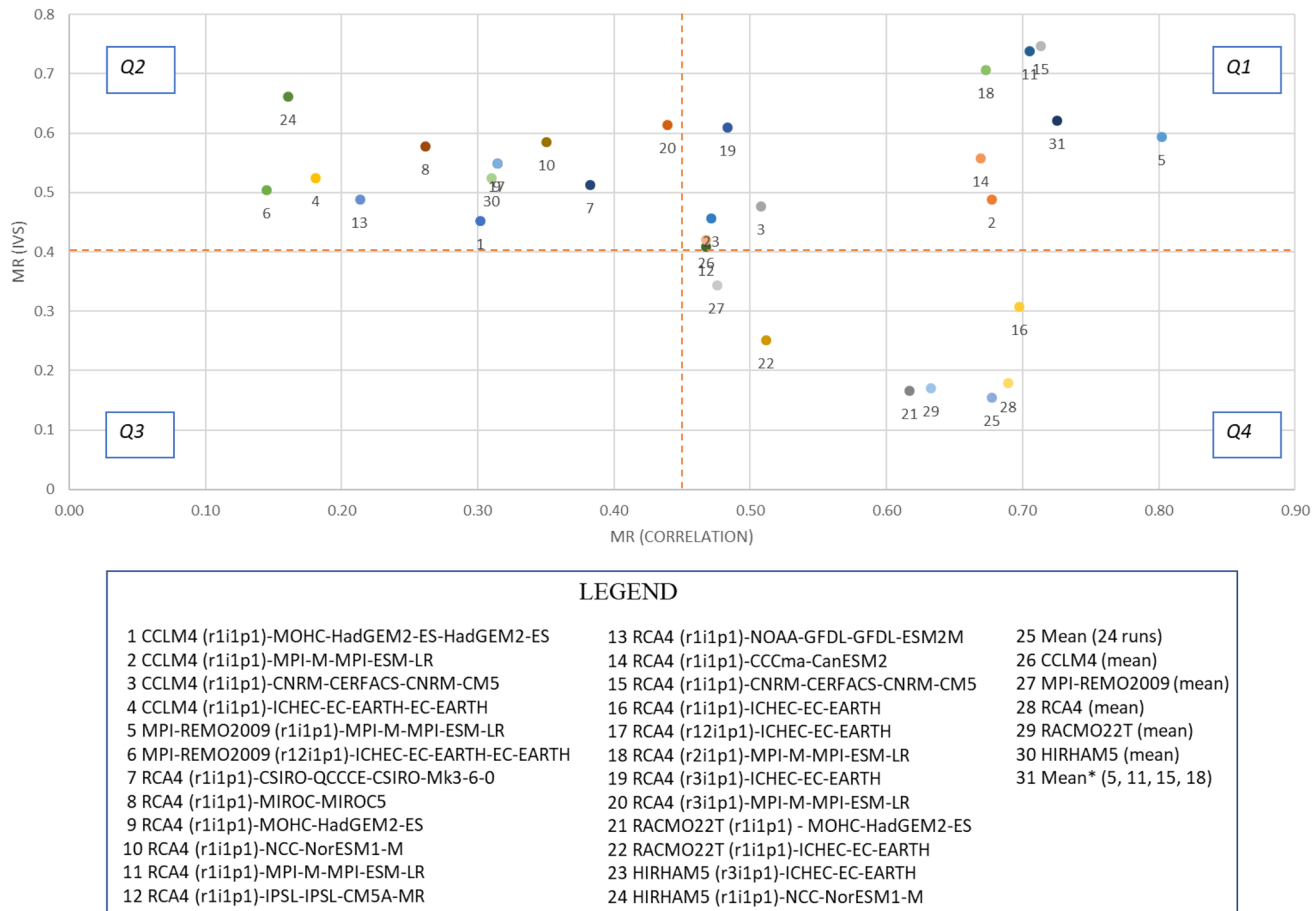
Institute	RCM	Ensemble	Driving model
Max Planck Institute (MPI), Germany	REMO2009	r1i1p1	MPI-M-MPI-ESM-LR
Sveriges Meteorologiska och Hydrologiska Institut (SMHI), Sweden	SMHI Rossby Center Regional Atmospheric Model (RCA4)	r1i1p1	MPI-M-MPI-ESM-LR
		r2i1p1	CNRM-CERFACS-CNRM-CM5 CCCMa-CanESM2 MPI-M-MPI-ESM-LR

**Table 4** As in Table 3 but with TAMSAT3 as reference dataset

Institute	RCM	Ensemble	Driving model
Max Planck Institute (MPI), Germany	REMO2009	r1i1p1	MPI-M-MPI-ESM-LR
Sveriges Meteorologiska och Hydrologiska Institut (SMHI), Sweden	SMHI Rossby Center Regional Atmospheric Model (RCA4)	r1i1p1	MPI-M-MPI-ESM-LR
		r2i1p1	CNRM-CERFACS-CNRM-CM5
Climate Limited-Area Modelling (CLM) Community	CLMcom COSMOCLM (CCLM4)	r1i1p1	MPI-M-MPI-ESM-LR

**Table 5** Top four model runs in simulating EA's precipitation characteristics (with both CHIRPS and TAMSAT3 as reference datasets)

Institute	RCM	Ensemble	Driving model
Max Planck Institute (MPI), Germany	REMO2009	r1i1p1	MPI-M-MPI-ESM-LR
Sveriges Meteorologiska och Hydrologiska Institut (SMHI), Sweden	SMHI Rossby Center Regional Atmospheric Model (RCA4)	r1i1p1 r2i1p1	MPI-M-MPI-ESM-LR CNRM-CERFACS-CNRM-CM5 MPI-M-MPI-ESM-LR

**Fig. 7** Same as Fig. 5 but incorporating an ensemble mean (Mean\*) of the top 4 model runs

west of Tanzania, Rwanda, Burundi and northern Uganda where a reduction of up-to 10 days in a year is projected. Our findings are consistent with general findings of recent studies in the study domain (i.e. Osima et al. 2018; Gudoshava et al. 2020) but show slight differences in details – possibly because the two studies computed the indices at seasonal timescales under global warming scenarios of 1.5 °C and 2.0 °C. The future changes in CDD and CWD could be as a result of a shift in general circulation patterns such as the El Nino Southern Oscillation (ENSO), the Indian Ocean Dipole (IOD) (Shonk et al. 2018; Endris et al. 2019). Future changes in the distribution and occurrence of precipitation have also been linked to changes in southward

and northward movement patterns of the intertropical convergence zone (ITCZ) over EA (Dunning, Black and Allan 2018). Projections show a decline in June to August (JJA) and MAM mean precipitation (Endris et al. 2019) hence increasing CDD events in the study domain.

Consistent with similar studies in our study domain (e.g. Shongwe et al. 2011; Vizy and Cook 2012; Dunning et al. 2018), our findings show an increase in SDII of up-to 2.5 mm/day (about 25%) over most of the study domain except for Burundi and northern Kenya, and east African coast where no significant changes are recorded. Increased CDD events, decreasing CWD events, the drying MAM and JJA seasons, and an increase in SDII imply a possibility

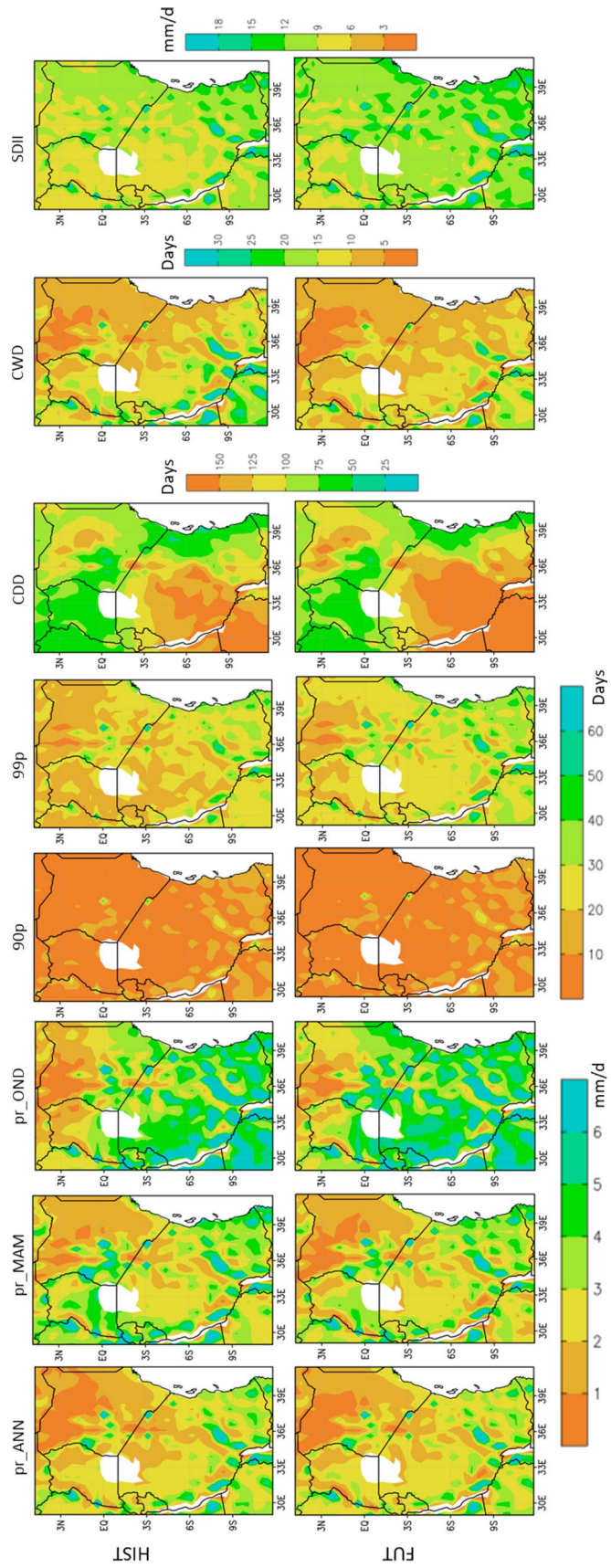


**Fig. 8** Future (FUT) and historical (HIST) climatology of precipitation descriptors using an ensemble mean of top four model runs under the RCP8.5 scenario. Water bodies are shown in white

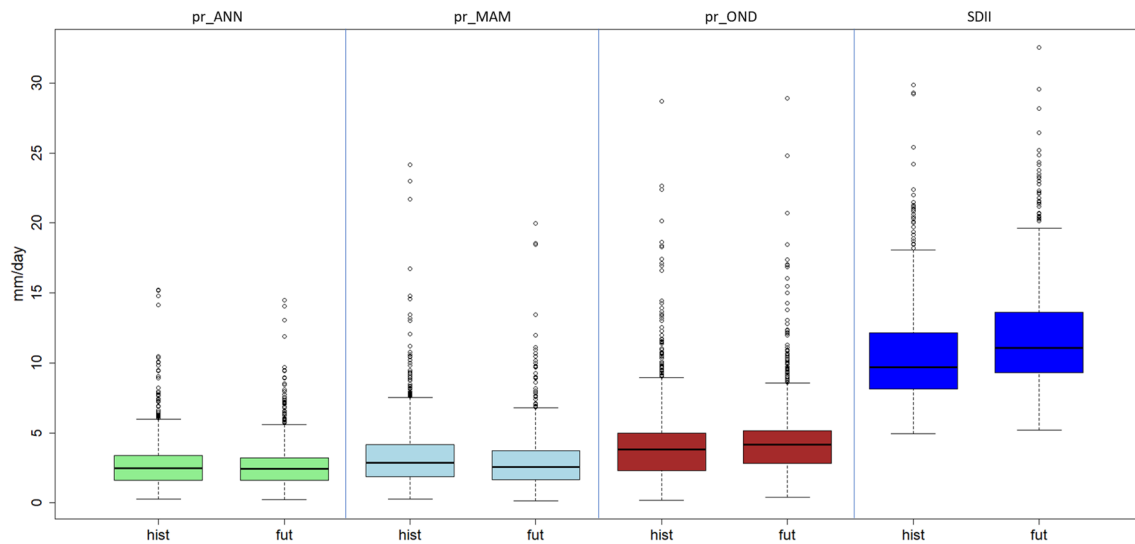


**Fig. 9** Box plots showing historical (hist) and future (fut) mean daily precipitation for ANN, MAM and OND, and SDII. The outliers represent grid-cells with projected changes exceeding  $1.5 \times$  Inter-Quartile Range (IQR) above the upper quartile

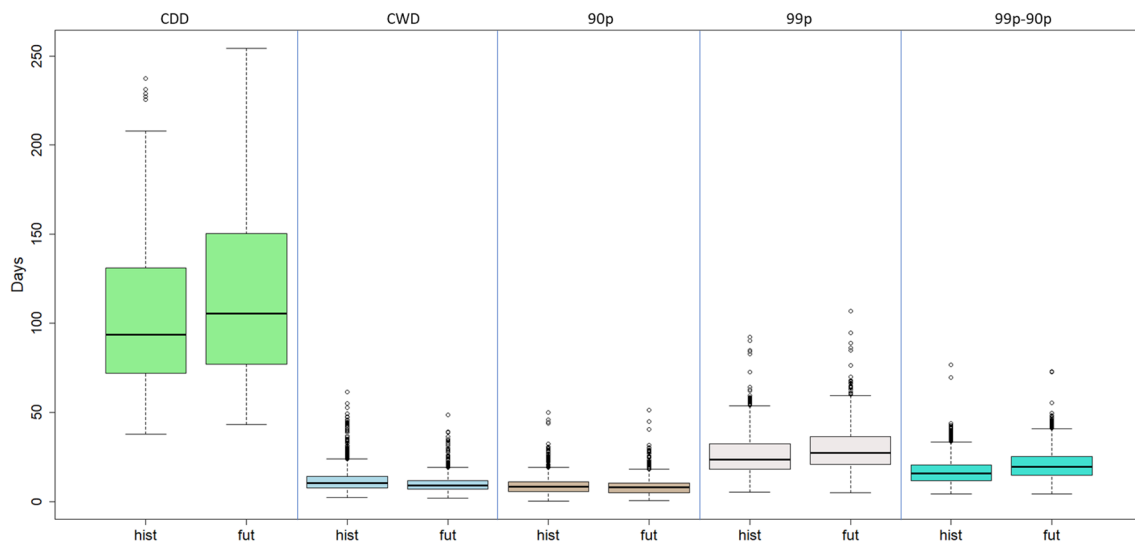


**Fig. 10** Same as Fig. 9 but for CDD, CWD, 90p, 99p, and 99p–90p

of fewer rainy days with above normal daily precipitation. This observation poses a threat to agricultural activities and, hence, socio-economic wellbeing in E. Africa whose economy is largely driven by rainfed smallholder farming (Salami et al. 2010; Alessandro et al. 2015).

Projections for very intense precipitation (99p) events show a general increase in most of the study domain except parts of northern Kenya and the EA coast where no significant changes are recorded. Some areas (e.g. central and northern Tanzania, Burundi and southern Kenya) record changes in 99p of up-to 10 days in a year. Projections for the width of the right tail of precipitation distribution (99p–90p)

show a general increase over the study area except parts of northern Kenya, central Uganda, and the EA coast. Areas over central and northern Tanzania record the highest increase of up-to 10 days (25%) in a year. Our results are consistent with findings from CMIP5 projections for E. Africa (Scoccimarro et al. 2013).

Given that projections for heavy precipitation events (90p) show no significant changes, it follows that E. Africa is likely to experience more intense precipitation (represented by 99p–90p) by the end of the twenty-first century. The results are consistent with increasing SDII, CDD, and mean daily precipitation (especially during OND) established in this study.

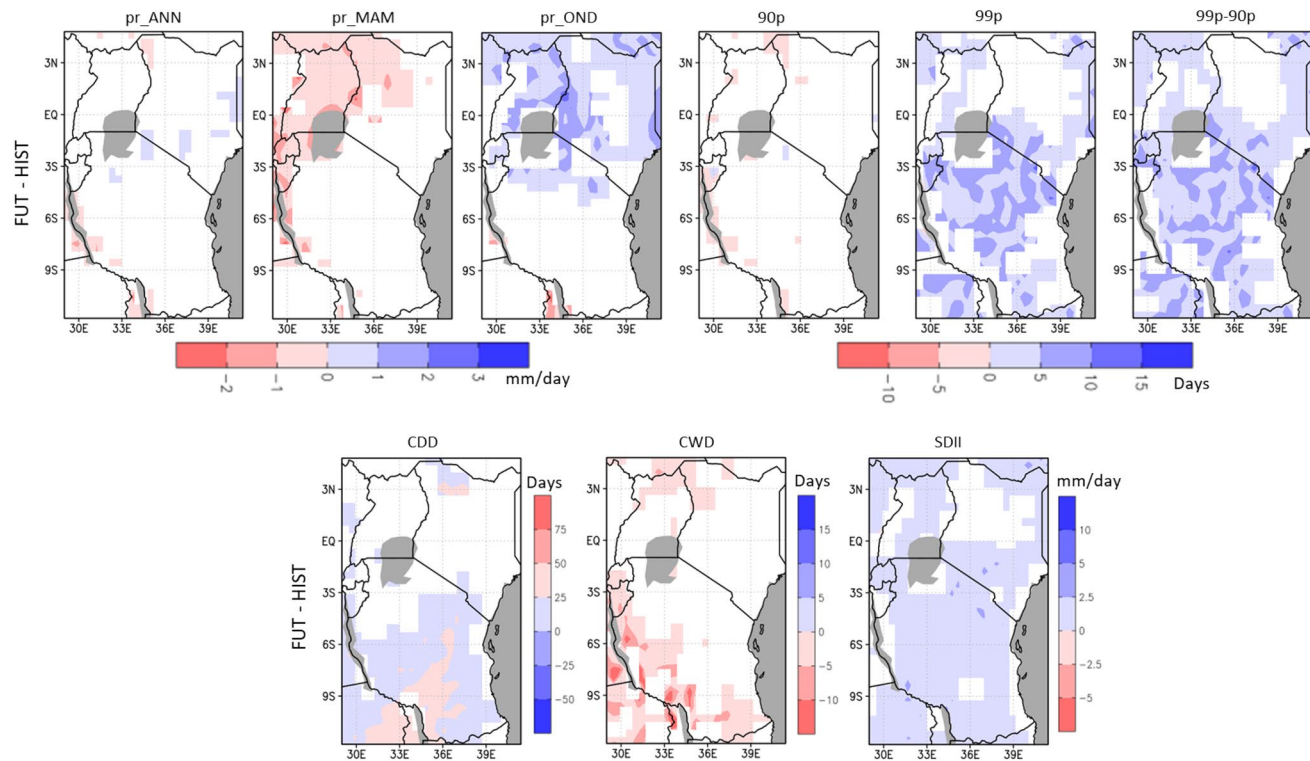


**Fig. 11** Future (2071–2099) precipitation changes (at 95% confidence level) over EA relative to the baseline (1977–2005). Water bodies are shown in grey

East Africa's economy is mainly supported by agriculture, tourism and related sectors which predominantly depend on rainfall (Alessandro et al. 2015; Hawinkel et al. 2016). Here, agriculture accounts for approximately 36% of East African Community (EAC)'s gross domestic product (GDP, AfDB 2018). About 80% of EAC's population draws its livelihood from agriculture (EAC 2018). In Kenya, for instance, agriculture accounts for more than a quarter of GDP, 65% of exports, 70% of rural jobs, and 60% of earnings from foreign exchange (Alessandro et al. 2015; FAO 2018). Yet, about 95% of farmed land in sub-Saharan Africa is rain-fed (Rockström et al. 2010; IWMI 2018). With the region already facing the impacts of a changing climate (Morton 2007; Ochieng et al. 2016; Mubiru et al. 2018), an increase in heavy and intense precipitation events in future is likely to adversely affect the socio-economic wellbeing of the region. Therefore, there is need for concerted effort from all actors in develop effective climate services to enhance the adaptive capacity of East Africans for sustainable socio-economic development in the face of the climate crisis.

#### 4 Summary and conclusions

First, an assessment of the performance of 24 simulations from 5 CORDEX RCMs (forced by CMIP5 GCMs) in simulating EA's precipitation characteristics was done using 8

descriptors of E. African precipitation (Table 2). Overall, RCA4 (r1i1p1) forced by CNRM-CERFACS-CNRM-CM5 and MPI-M-MPI-ESM-LR, REMO2009 (r1i1p1) forced by MPI-M-MPI-ESM-LR, and RCA4 (r2i1p1) forced by MPI-M-MPI-ESM-LR emerged as the top 4 model runs in simulating both spatial and temporal characteristics of precipitation over EA. Contrary to earlier studies (e.g. Nikulin et al. 2012; Endris et al. 2013; Kisembe et al. 2018) that showed that a multi-model ensemble mean could sufficiently simulate EA's precipitation characteristics, our results show that a multi-model ensemble (for a large number of ensemble members) perform dismally when assessed against a big set of criteria compared to a smaller ensemble mean of the top performing models. In our case, an ensemble mean of top four model runs outperformed an ensemble mean of 24 model simulations and ensemble means for all runs in an RCM. Of the top four model simulations, three are from the RCA4 model while the other is from the REMO2009 model.

Consistent with recent studies in the study area that have shown a decrease/increase in future mean MAM/OND precipitation (e.g. Endris et al. 2019), our results show a reduction/increase in mean daily precipitation for MAM/OND for the period 2071–2099. Our findings also show an increase/decrease in CDD/CWD events in the study domain consistent with similar studies (e.g. Osima et al. 2018; Wainwright et al. 2019; Gudoshava et al. 2020). Projections for SDII as

well as the width of the right tail of the precipitation distribution (99p–90p) show an increase in most parts of the study domain. An increase in SDII and 99p–90p implies a potential for heavy and extreme precipitation incidences by end of the twenty-first century relative to the baseline (1977–2005).

Given that human and natural systems are, generally, affected by heavy and extreme precipitation (Giorgi et al. 2011; Niang et al. 2014), projected changes in heavy and extreme precipitation events (especially during the OND season) necessitate proactive mitigation and adaptation strategies for sustainability in the region. Building the adaptive capacity of smallholder farmers, hitherto dependent on rain-fed subsistence farming, to shift to climate-smart agriculture could boost the region's agricultural productivity under the projected conditions and, hence, socio-economic development. However, more research is required to monitor the changes with time and inform development and adaptation strategies for sustainability.

**Acknowledgements** The authors wish to thank colleagues from the IGAD Climate Prediction and Applications Centre (ICPAC), The African Academy of Sciences (AAS), and Kenyatta University, Nairobi for their insights that helped shape this paper. Contribution of various modelling groups participating in CORDEX as outlined in Table 1 (as well CHIRPS and TAMSAT data) are acknowledged for making the data publicly available. Further, the lead author acknowledges the contribution of Dr. Benjamin Gyampoh towards the realization of this paper. Statements made and errors, if any, are solely the responsibility of the authors and not the institutions they represent.

**Funding** This research did not receive any specific grant from funding agencies in the public, commercial, or not-for-profit sectors.

## References

- AfDB (2018) East Africa Economic Outlook 2018. The African Development Bank Group. <https://bit.ly/2Beg1fm>
- Alessandro SD, Caballero J, Simpkin S, Lichte J (2015) Kenya Agricultural Risk Assessment. The World Bank. <https://bit.ly/2RnCyhP>
- Beck HE, Wood EF, Pan M, Fisher CK, Miralles DG, van Dijk AI, McVicar TR, Adler RF (2019) MSWEP V2 global 3-hourly 0.1° precipitation: methodology and quantitative assessment. *Bull Am Meteorol Soc* 100:473–500. <https://doi.org/10.1175/BAMS-D-17-0138.1>
- Breil M, Panitz HJ, Schädler G (2017) Impact of soil-vegetation-atmosphere interactions on the spatial precipitation distribution in the Central Sahel. *Meteorol Z* 26(4):379–389. <https://doi.org/10.1127/metz/2017/0819>
- Camberlin P (2018) Climate of eastern Africa. *Oxf Res Encycl Clim Sci*. <https://doi.org/10.1093/acrefore/9780190228620.013.512>
- Chen W, Jiang Z, Li L (2011) Probabilistic projections of climate change over China under the SRES A1B scenario using 28 AOGCMs. *J Clim* 24:4741–4756. <https://doi.org/10.1175/2011jcli4102.1>
- Cook KH, Vizy EK (2013) Projected changes in east African rainy seasons. *J Clim* 26(16):5931–5948. <https://doi.org/10.1175/JCLI-D-12-00455.1>
- Déqué M, Calmant S, Christensen OB, Aquilla AD, Maule CF, Haensler A, Nikulin G, Teichmann C (2017) A multi-model climate response over tropical Africa at + 2 °C. *Clim Serv* 7:87–95. <https://doi.org/10.1016/j.ciser.2016.06.002>
- Diaconescu EP, Gachon P, Laprise R (2015) On the remapping procedure of daily precipitation statistics and indices used in regional climate model evaluation. *J Hydrometeorol* 16:2301–2310. <https://doi.org/10.1175/jhm-d-15-0025.1>
- Dinku T, Funk C, Peterson P, Maidment R, Tadesse T, Gadain H, Ceccato P (2018) Validation of the CHIRPS satellite precipitation estimates over Eastern Africa. *Q J R Meteorol Soc* 144:292–312. <https://doi.org/10.1002/qj.3244>
- Dosio A, Jones RG, Jack C, Lennard C, Nikulin G, Hewitson B (2019) What can we know about future precipitation in Africa? Robustness, significance and added value of projections from a large ensemble of regional climate models. *Clim Dyn* 53(9–10):5833–5858. <https://doi.org/10.1007/s00382-019-04900-3>
- Dosio A, Panitz HJ (2016) Climate change projections for CORDEX-Africa with COSMO-CLM regional climate model and differences with the driving global climate models. *Clim Dyn* 46(5–6):1599–1625. <https://doi.org/10.1007/s00382-015-2664-4>
- Dunning CM, Black E, Allan RP (2018) Later wet seasons with more intense precipitation over Africa under future climate change. *J Clim* 31(23):9719–9738. <https://doi.org/10.1175/JCLI-D-18-0102.1>
- EAC (2018) Investment in agriculture. East African Community. <https://bit.ly/2Tlsqo6>
- Endris HS, Lennard C, Hewitson B, Dosio A, Nikulin G, Artan GA (2019) Future changes in precipitation associated with ENSO, IOD and changes in the mean state over Eastern Africa. *Clim Dyn* 52(3–4):2029–2053. <https://doi.org/10.1007/s00382-018-4239-7>
- Endris HS, Omondi P, Jain S, Lennard C, Hewitson B, Changa L, Awange JL, Dosio A, Ketiem P, Nikulin G, Panitz HJ, Büchner M, Stordal F, Tazalika L (2013) Assessment of the performance of CORDEX regional climate models in simulating East African precipitation. *J Clim* 26:8453–8475. <https://doi.org/10.1175/JCLI-D-12-00708.1>
- FAO (2018) The agriculture sector in Kenya. Food and Agriculture Organization of the United Nations. <https://bit.ly/2QdVZGQ>
- Favre A, Stone D, Cerezo R, Philippon N, Abiodun B (2011) Diagnostic of monthly precipitation from CORDEX simulations over Africa: focus on the annual cycles. In: Proceedings of the international conference on the coordinated regional climate downscaling experiment—CORDEX, Trieste, Italy. World Climate Research Program. <https://bit.ly/2CHeZJQ>
- Funk C, Peterson P, Landsfeld M, Pedreros D, Verdin J, Shukla S, Husak G, Rowland J, Harrison L, Hoell A, Michaelsen J (2015) The climate hazards infrared precipitation with stations—a new environmental record for monitoring extremes. *Sci Data* 2:150066. <https://doi.org/10.1038/sdata.2015.66>
- Gebrechorkos SH (2019) Changes in temperature and precipitation extremes in Ethiopia. *Int J Climatol* 39:18–30. <https://doi.org/10.1002/joc.5777>
- Giorgi F, Im ES, Coppola E, Diffenbaugh NS, Gao XJ, Mariotti L, Shi Y (2011) Higher hydroclimatic intensity with global warming. *J Clim* 24:5309–5324. <https://doi.org/10.1175/2011jcli3979.1>
- Gudoshava M, Misiani HO, Segele ZT, Jain S, Ouma JO, Otieno G, Anyah R, Indasi VS, Endris HS, Osima S, Lennard C, Zaroug M, Mwangi E, Nimusima A, Kondowe A, Ogwang B, Artan G, Atheru Z (2020) Projected effects of 1.5 °C and 2 °C global warming levels on the intra-seasonal precipitation characteristics over the Greater Horn of Africa. *Environ Res Lett* 15(3):034037. <https://doi.org/10.1088/1748-9326/ab6b33>
- Hawinkel P, Thiery W, Lhermitte S, Swinnen E, Verbist B, Van Orshoven J, Muys B (2016) Vegetation response to precipitation variability in East Africa controlled by biogeographical factors. *J Geophys Res* 121:2422–2444

- Huffman GJ, Adler RF, Bolvin DT, Gu G (2009) Improving the global precipitation record: GPCP version 2.1. *Geophys Res Lett* 36:L17808. <https://doi.org/10.1029/2009GL040000>
- IWMI (2018) Rainfed agriculture. International Water Management Institute. <https://bit.ly/2OhzKCy>
- Jiang Z, Li W, Xu J, Li L (2015) Extreme precipitation indices over China in CMIP5 models. Part I: Model evaluation. *J Clim* 28:8603–8619. <https://doi.org/10.1175/jcli-d-15-0099.1>
- Kilavi M, MacLeod D, Ambani M, Robbins J, Dankers R, Graham R, Titley H, Salih AAM, Todd MC (2018) Extreme precipitation and flooding over central Kenya including Nairobi city during the long-rains season 2018: causes, predictability, and potential for early warning and actions. *Atmosphere* 9:472. <https://doi.org/10.3390/atmos9120472>
- Kim J, Waliser DE, Mattmann CA, Goodale CE, Hart AF, Zimdars PA, Crichton DJ, Jones C, Nikulin G, Hewitson B, Jack C, Lennard C, Favre A (2014) Evaluation of the CORDEX-Africa multi-RCM hindcast: systematic model errors. *Clim Dyn* 42:1189–1202. <https://doi.org/10.1007/s00382-013-1751-7>
- Kiros G, Shetty A, Nandagiri L (2017) Extreme precipitation signatures under changing climate in semi-arid northern highlands of Ethiopia. *Cogent Geosci* 3(1):1–20. <https://doi.org/10.1080/23312041.2017.1353719>
- Kisembe J, Dosio A, Lennard C, Sabiiti G, Nimusimma A, Favre A (2018) Evaluation of precipitation simulations over Uganda in CORDEX regional climate models. *Theor Appl Climatol* 137:1117–1134. <https://doi.org/10.1007/s00704-018-2643-x>
- Lazenby MJ, Todd MC, Chadwick R, Wang Y (2018) Future precipitation projections over central and Southern Africa and the adjacent Indian Ocean: what causes the changes and the uncertainty? *J Clim* 31(12):4807–4826. <https://doi.org/10.1175/JCLI-D-17-0311.1>
- Maidment R, Grimes D, Black E, Tarnavsky E, Young M, Greatrex H, Allan RP, Stein T, Nkonde E, Senkunda S, Alcántara EMU (2017) A new, long-term daily satellite-based precipitation dataset for operational monitoring in Africa. *Sci Data* 4:170063. <https://doi.org/10.1038/sdata.2017.63>
- Meehl GA, Bony S (2011) Introduction to CMIP5. CLIVAR exchanges, no. 56. International CLIVAR Project Office, Southampton, pp 4–5
- Menne MJ, Durre I, Vose RS, Gleason BE, Houston TG (2012) An overview of the global historical climatology network-daily database. *J Atmos Oceanic Technol* 29:897–910. <https://doi.org/10.1175/JTECH-D-11-00103.1>
- Morton JF (2007) The impact of climate change on smallholder and subsistence agriculture. *Proc Natl Acad Sci USA* 104(50):19680–19685. <https://doi.org/10.1073/pnas.0701855104>
- Moss RH, Edmonds JA, Hibbard KA, Manning MR, Rose SK, van Vuuren DP, Carter TR, Emori S, Kainuma M, Kram T, Meehl GA, Mitchell JFB, Nakicenovic N, Riahi K, Smith SJ, Stouffer RJ, Thomson AM, Weyant JP, Wilbanks TJ (2010) The next generation of scenarios for climate change research and assessment. *Nature* 463:747–756. <https://doi.org/10.1038/nature08823>
- Mubiru DN, Radeny M, Kyazze FB, Zziwa A, Lwasa J, Kinyangi J, Mungai C (2018) Climate trends, risks and coping strategies in smallholder farming systems in Uganda. *Clim Risk Manag* 22:4–21. <https://doi.org/10.1016/j.crm.2018.08.004>
- Muhati GL, Olago D, Olaka L (2018) Past and projected precipitation and temperature trends in a sub-humid Montane Forest in Northern Kenya based on the CMIP5 model ensemble. *Global Ecol Conserv* 16:e00469. <https://doi.org/10.1016/j.gecco.2018.e00469>
- Niang I, Ruppel OC, Abdrabo MA, Essel A, Lennard C, Padgham J, Urquhart P (2014) Africa. In: Barros VR, Field CB, Dokken DJ, Mastrandrea MD, Mach KJ, Bilir TE, Chatterjee M, Ebi KL, Estrada YO, Genova RC, Girma B, Kissel ES, Levy AN, MacCracken S, Mastrandrea PR, White LL (eds.) *Climate change 2014: impacts, adaptation, and vulnerability. Part B: Regional aspects. Contribution of Working Group II to the fifth assessment report of the intergovernmental panel on climate change*. Cambridge University Press, Cambridge, pp 1199–1265
- Nicholson SE (2017) Climate and climatic variability of precipitation over eastern Africa. *Rev Geophys* 55(3):590–635. <https://doi.org/10.1002/2016RG000544>
- Nicholson SE, Kim J (1997) The relationship of the el nino oscillation to African precipitation. *Int J Climatol* 17:117–135. [https://doi.org/10.1002/\(SICI\)1097-0088\(199702\)17:2%3c117:AID-JOC84%3e3.0.CO;2-O](https://doi.org/10.1002/(SICI)1097-0088(199702)17:2%3c117:AID-JOC84%3e3.0.CO;2-O)
- Nikulin G, Jones C, Giorgi F, Asrar G, Büchner M, Cerezo-Mota R, Christensen OB, Déqué M, Fernandez J, Hänsler A, van Meijgaard E, Samuelsson P, Sylla MB, Sushama L (2012) Precipitation climatology in an ensemble of CORDEX-Africa regional climate simulations. *J Clim* 25:6057–6078. <https://doi.org/10.1175/jcli-d-11-00375.1>
- Ochieng J, Kirim L, Mathenge M (2016) Effects of climate variability and change on agricultural production: The case of small-scale farmers in Kenya. *NJAS Wageningen J Life Sci* 77:71–78. <https://doi.org/10.1016/j.njas.2016.03.005>
- Otega OM (2017) Use of scientific and indigenous knowledge in adapting to climate change and variability at the Kenyan coast. Master's thesis, University of Nairobi
- Omondi PA, Awange JL, Forootan E, Ogallo LA, Barakiza R, Girmaw GB, Fesseha I, Kululeteria V, Kilembe C, Mbati MM, Kilavi M, King'uyu SM, Omey PA, Njogu A, Badr EM, Musa TA, Muchiri P, Bamanya D, Komutunga E (2014) Changes in temperature and precipitation extremes over the Greater Horn of Africa region from 1961 to 2010. *Int J Climatol* 34(4):1262–1277. <https://doi.org/10.1002/joc.3763>
- Opiyo FE, Wasonga OV, Nyangito MM (2014) Measuring household vulnerability to climate-induced stresses in pastoral rangelands of Kenya: implications for resilience programming. *Pastoralism* 4:10. <https://doi.org/10.1186/s13570-014-0010-9>
- Osima S, Indasi VS, Zaroug M, Endris HS, Gudoshava M, Misiani HO, Nimusimma A, Anyah RO, Otieno G, Ogwang BA, Jain S, Kondowe AL, Mwangi E, Lennard C, Grigory N, Dosio A (2018) Projected climate over the Greater Horn of Africa under 1.5 °C and 2 °C global warming. *Environ Res Lett* 13:065004. <https://doi.org/10.1088/1748-9326/aaba1b>
- Peterson TC, Folland C, Gruza G, Hogg W, Mokssit A, Plummer N (2001) Report of the activities of the Working Group on Climate Change Detection and related rapporteurs. In: World Meteorology Organisation technical document 1071, 143 pp, Commission for Climatology, World Meteorology Organisation, Geneva
- Rockström J, Karlberg L, Wani SP, Barron J, Hatibu N, Oweis T, Bruggeman A, Farahani J, Qiang Z (2010) Managing water in rainfed agriculture—the need for a paradigm shift. *Agric Water Manag* 97:543–550. <https://doi.org/10.1016/j.agwat.2009.09.009>
- Salami A, Kamara AB, Brixiova Z (2010) Smallholder agriculture in East Africa: trends, constraints and opportunities smallholder agriculture in East Africa. African Development Bank Group working paper no. 105, January
- Scoccimarro E, Gualdi S, Bellucci A, Zampieri M, Navarra A (2013) Heavy precipitation events in a warmer climate: results from CMIP5 models. *J Clim* 26:7902–7911. <https://doi.org/10.1175/jcli-d-12-00850.1>
- Scoccimarro E, Gualdi S, Bellucci A, Zampieri M, Navarra A (2016) Heavy precipitation events over the Euro-Mediterranean region in a warmer climate: results from CMIP5 models. *Reg Environ Change*. <https://doi.org/10.1007/s10113-014-0712-y>
- Shiferaw A, Tadesse T, Rowe C, Oglesby R (2018) Precipitation extremes in dynamically downscaled climate scenarios over the greater horn of Africa. *Atmosphere* 9(3):1–28. <https://doi.org/10.3390/atmos9030112>

- Shongwe ME, van Oldenborgh GJ, van den Hurk B, van Aalst M (2011) Projected changes in mean and extreme precipitation in Africa under global warming. Part II: East Africa. *J Clim* 24(14):3718–3733. <https://doi.org/10.1175/2010JCLI2883.1>
- Shonk JKP, Guilyardi E, Toniazzo T, Woolnough SJ, Stockdale T (2018) Identifying causes of Western Pacific ITCZ drift in ECMWF system 4 hindcasts. *Clim Dyn* 50(3–4):939–954. <https://doi.org/10.1007/s00382-017-3650-9>
- Sillmann J, Kharin VV, Zwiers FW, Zhang X, Branaugh D (2013) Climate extremes indices in the CMIP5 multimodel ensemble: Part 2. Future climate projections. *J Geophys Res Atmos* 118:2473–2493. <https://doi.org/10.1002/jgrd.50188>
- Vizy EK, Cook KH (2012) Mid-twenty-first-century changes in extreme events over northern and tropical Africa. *J Clim* 25(17):5748–5767. <https://doi.org/10.1175/JCLI-D-11-00693.1>
- Wainwright CM, Marsham JH, Keane RJ, Rowell DP, Finney DL, Black E, Allan RP (2019) Eastern African paradox' precipitation decline due to shorter not less intense long rains. *Clim Atmos Sci* 2(1):1–9. <https://doi.org/10.1038/s41612-019-0091-7>
- Zhou B, Wen QH, Xu Y, Song L, Zhang X (2014) Projected changes in temperature and precipitation extremes in China by the CMIP5 multimodel ensembles. *J Clim* 27:6591–6611. <https://doi.org/10.1175/jcli-d-13-00761.1>
- Zhou RG, Hu W, Fan P, Ian H (2017) Quantum realization of the bilinear interpolation method for NEQR. *Sci Rep* 7:1. <https://doi.org/10.1038/s41598-017-02575-6>

**Publisher's Note** Springer Nature remains neutral with regard to jurisdictional claims in published maps and institutional affiliations.